

On the discrete Peyrard-Bishop model of DNA: stationary solutions and stability

Sara Cuenda* and Angel Sánchez*,†

**Grupo Interdisciplinar de Sistemas Complejos (GISC) and Departamento de Matemáticas
Universidad Carlos III de Madrid, Avenida de la Universidad 30,*

28911 Leganés, Madrid, Spain‡ and

†*Instituto de Biocomputación y Física de Sistemas Complejos (BIFI),
Facultad de Ciencias, Universidad de Zaragoza, 50009 Zaragoza, Spain*

(Dated: November 4, 2018)

Abstract

As a first step in the search of an analytical study of mechanical denaturation of DNA in terms of the sequence, we study stable, stationary solutions in the discrete, finite and homogeneous Peyrard-Bishop DNA model. We find and classify all the stationary solutions of the model, as well as analytic approximations of them, both in the continuum and in the discrete limits. Our results explain the structure of the solutions reported by Theodorakopoulos *et al.* [Phys. Rev. Lett. **93**, 258101 (2004)] and provide a way to proceed to the analysis of the generalized version of the model incorporating the genetic information.

PACS numbers: 87.10.+e, 05.45.-a, 02.60.Lj

Keywords: DNA; discrete limit; stationary states; stability of solutions

*Electronic address: scuenda@math.uc3m.es

†Electronic address: anxo@math.uc3m.es

‡URL: <http://gisc.uc3m.es>

LEAD PARAGRAPH

DNA, the molecule that constitutes the basis of the genetic code, is of utmost importance. In particular, its mechanical properties are crucial as opening the double helix structure of DNA is needed to read the genetic code and for replication of the molecule for reproduction. The complete separation of the double helix is called replication, and can be achieved by heating or mechanically, by pulling the two strands of the molecule apart. We here address the mathematical description of mechanical denaturation in terms of a simple model. We determine and classify the solutions of the model equations and study their stability properties. We also provide an approximate but very accurate way to deal analytically with those solutions. Beyond mechanical features, our results are relevant for studies of the thermodynamic properties of the DNA chain, and may have genomic applications, in so far as mechanical denaturation experiments that give information about DNA composition can be modelled by our model and solutions.

I. INTRODUCTION

Nonlinear models appear in many fields of science since the pioneering discoveries, almost 50 years ago, of Fermi, Pasta and Ulam [1]. This work, in the field of physics, has led many scientist to use nonlinear models in the study of complex systems [2] in other subjects. Nonlinear models entered into DNA physics with Englander and co-workers [3] (see [4] for a review on nonlinear models of DNA), in 1980, when they modeled the dynamics of DNA with a sine-Gordon equation. Since then, a lot of work has been devoted to nonlinear excitations in DNA, both from the dynamics and the statistical mechanics points of view. Among this body of work, a particularly succesful model is the Peyrard-Bishop (PB) one [5, 6], that will be our starting point in this paper.

One problem of special interest in the framework of DNA was the thermal denaturation transition, which takes place at temperatures around 90°C, when the two strands of the DNA molecule separate. On the other hand, mechanical denaturation, that occurs when one of the strands of the molecule is separated from the other by pulling it in single molecule experiments, was achieved in the last few years [7]. In order to model these phenomena, most of the research done so far refers to *homopolymers*, i.e., homogeneous DNA molecules consisting entirely of A-T or C-G base pairs. When the issue under discussion is genomics, or gene identification, which is very much related to the above mentioned problems, models of *heteropolymers* are required: The distribution of A-T and C-G base pairs follows non-uniform, nonhomogeneous sequences obtained from genome analysis. The heterogeneous PB model is also being used for identifying relevant sites, such as promoters [8, 9] in viral sequences, and also for analyzing the thermal denaturation process [10].

The main motivation of this work is the study of the effects of the sequence heterogeneity on the dynamics of the mechanical denaturation process. We began that research program by analyzing the Englander (basically, the sine-Gordon equation [2]) model. The results we obtained [11, 12] showed that the Englander model was much too simple to reproduce the phenomena observed in experiments, and therefore we decided to focus on the PB model (see [13] for an authoritative review about this model). In that context, our immediate aim was to obtain a tool in this model similar the effective potential proposed for the Englander model by Salerno and Kivshar [14, 15, 16] in order to study the relation between the dynamics of these excitations and gene identification. To that end, it is necessary to obtain stationary

states of the homogeneous model. Those were available for the continuous version of the PB model, but, in fact, DNA is quite a discrete system, and the discretization parameter depends on experimental measurements used as parameters in the model. For instance, in the PB model, the dimensionless parameter that defines the effective discretization of the system can go from $R = 10.1$ (see next section for a definition of R), used in [13, 17], to $R \simeq 75$ used in [18], or even to $R = 100$ in [19]. In all cases, these R values correspond to systems that are far from the continuum limit. Therefore, as a first step towards our chief goal of understand sequence effects on denaturation, our immediate purpose is to study stable, stationary states in the discrete PB model, with a special focus on their dependence on the effective discretization.

In this paper, we aim to finding stationary solutions of the PB model and their corresponding stability conditions. These issues are addressed in Secs. II. Subsequently, we discuss the validity of the continuum limit and the domain wall approximation in Sec. III, while in the main part of the paper, Sec. IV, we propose analytical approximations for the discrete case and compare our results with the ones obtained in [17]. Finally, Sec. V concludes the paper by summarizing our main results and their possible implications.

II. DISCRETE SOLUTIONS AND STABILITY

In the following we will use the dimensionless PB model, defined by the hamiltonian

$$H = \sum_{n=0}^{N-1} \left\{ \frac{1}{2} \dot{Y}_n^2 + \frac{1}{2R} (Y_{n+1} - Y_n)^2 + V(Y_n) \right\}, \quad (1)$$

where $V(Y) = (1 - e^{-Y})^2$ is the Morse potential, that stands for the attraction between the two bases of a base pair, and R is a positive, dimensionless constant that refers to the intensity of the coupling of two consecutive bases. This constant plays the role of an effective discretization, $a = \sqrt{R}$, so that $R \gg 1$ stands for a large discretization and $R \ll 1$ is the continuous limit.

Static solutions of hamiltonian (1) must satisfy $\partial H / \partial Y_n = 0$, which turns out to be the recurrence relation

$$Y_{n+1} = 2Y_n - Y_{n-1} + RV'(Y_n), \quad (2)$$

for $n = 1, 2, \dots, N$. These solutions are uniquely defined by the initial condition $\{Y_0, Y_1\}$. If we restrict ourselves to solutions with $Y_0 = 0$, which we can do without loss of generality,

then each Y_n will only depend on the value $Y_1 = y$, so that Eq. (2) can be rewritten in terms of y introducing the notation $Y_n(y)$ instead of Y_n . From now on we will discuss the behavior of the solutions $Y_n(y)$ as a function of y .

Equation (2) describes stable and unstable solutions of hamiltonian (1). In order to assess the stability properties of the solutions, we need to study the hessian of the system,

$$\mathcal{H}_N(y) = \begin{pmatrix} d_1(y) & -1 & 0 & \dots & 0 \\ -1 & d_2(y) & -1 & \dots & 0 \\ 0 & -1 & d_3(y) & \dots & 0 \\ \vdots & \vdots & \vdots & \ddots & \vdots \\ 0 & 0 & 0 & \dots & d_N(y) \end{pmatrix}, \quad (3)$$

where $d_n(y) = 2 + RV''(Y_n(y))$, in order to find out the stability of solutions. Calling $\Delta_n(y)$ the determinant of the principal minor of order n of the hessian $\mathcal{H}_N(y)$, i.e.,

$$\Delta_n(y) = \det(\mathcal{H}_n(y)), \quad (4)$$

a stable solution must satisfy $\Delta_n(y) > 0$ for all $n = 1, 2, \dots, N$. As the hessian is a tridiagonal matrix, there is a recursive relation between different Δ_n ,

$$\Delta_{n+1}(y) = d_{n+1}(y)\Delta_n(y) - \Delta_{n-1}(y), \quad (5)$$

with $\Delta_1 = d_1$ and $\Delta_2 = d_1d_2 - 1$.

Expression (5) above can be rewritten in terms of $Y'_n(y)$. By deriving expression (2) with respect to y we find:

$$Y'_{n+1}(y) = \frac{dY_{n+1}(y)}{dy} = [2 + RV''(Y_n(y))]Y'_n(y) - Y'_{n-1}(y) = d_n(y)Y'_n(y) - Y'_{n-1}(y), \quad (6)$$

with $Y'_2(y) = \Delta_1(y)$ and $Y'_3(y) = \Delta_2(y)$. Therefore, it has to be

$$\Delta_n(y) = Y'_{n+1}(y), \quad (7)$$

for $n = 1, 2, \dots, N$, and hence the stability region of solutions (2) are the points that satisfy $Y'_n(y) > 0$ for all $n = 2, 3, \dots, N + 1$.

This far, no approximations were needed to obtain these results, still valid for any $V(Y)$. From now on, we will focus on the PB model by choosing the Morse potential as our $V(Y)$, in order to search for an analytic expression of the solutions (2), as well as to find the stability in terms of the initial condition y .

III. CONTINUUM LIMIT OF THE PEYRARD-BISHOP MODEL

This limit corresponds to taking $R \ll 1$, which means that we can use the approximation $Y_n(y) \rightarrow Y_{cont}(x, y)$ with $x = n\sqrt{R}$ in Eq. (2). By so doing we obtain the following differential equation:

$$\frac{\partial^2 Y_{cont}}{\partial x^2} = \frac{dV}{dY_{cont}}, \quad (8)$$

which can be easily solved using the initial conditions $Y_{cont}(x_0, y) = 0$ and $\partial Y_{cont}(x_0, y)/\partial x = y/\sqrt{R}$, where x_0 stands for the initial site of the model. This solution is

$$e^{Y_{cont}(x,y)} = \frac{y\sqrt{\frac{2}{R}} \sinh \left[\sqrt{2 + \frac{y^2}{R}}(x - x_0) + \sinh^{-1} \left(\frac{y}{\sqrt{2R}} \right) \right] + 2}{2 + \frac{y^2}{R}} \quad (9)$$

for $x \geq x_0$. Looking at expression (9) we see that, for a finite system, taking $y = 0$ implies $Y_{cont}(x, 0) = 0$ for all $x \geq x_0$. This result differs from the domain wall obtained in the continuum limit in the PB model [13] because in this case we have restricted ourselves to finite systems ($x \geq x_0$). For infinite systems, letting $Y_{cont}(x_0, y) \rightarrow 0$ as $x_0 \rightarrow \infty$, it can be seen that there is another stationary solution, namely

$$e^{Y(x)} = 1 + e^{\sqrt{2}x}, \quad (10)$$

In this respect, we believe that this solution should not be used as an approximation of a finite system because it is not a critical point of the continuum version of Eq. (1) and, therefore, we cannot speak of stability in this case as long as we consider DNA as a finite lattice.

An important feature of the continuum approximation is that, in Eq. (9), Y_{cont} can be written as a function of x and ξ , where $\xi = y/\sqrt{R}$. This implies a scaling relation between these two parameters, a relation that is absent for solutions of the discrete limit. This behavior can be seen in Fig. 1, where we represent Y_{cont} with respect to x (with $x_0 = 0$) for two values of ξ , compared to the exact result $Y_n(y)$ (recall that $x = n\sqrt{R}$) for different values of R , and with $y = \xi\sqrt{R}$. We clearly observe that for the largest values of R ($R = 1$ and, mostly, $R = 10$) the scaling relation is not fulfilled, indicating the crossover to the discrete limit regime.

To analyze the stability of these solutions, using the result of section II, it is enough to study the sign of $\partial Y_{cont}(x, y)/\partial y$ for all $x \geq 0$. As the derivative of expression (9) is quite

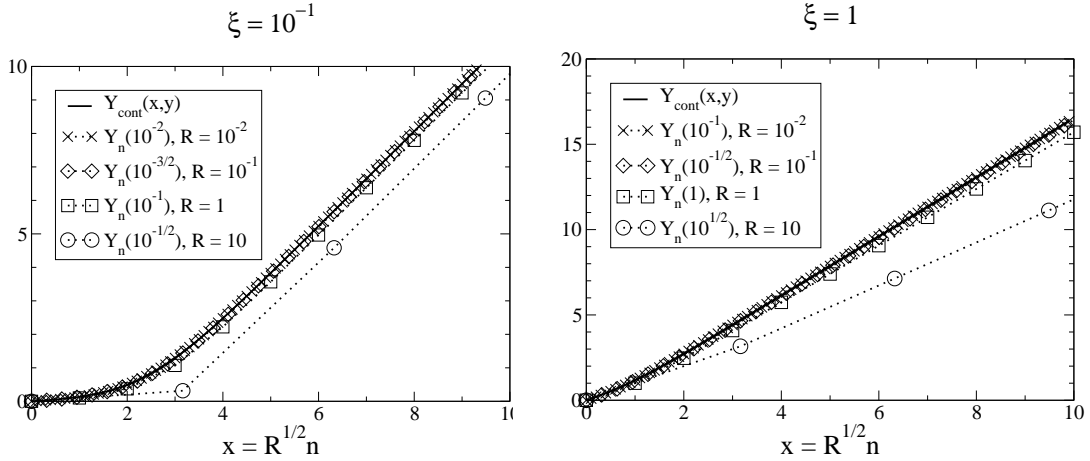


FIG. 1: Plots of $Y_{cont}(x, y)$ (obtained from expression (9)) for $\xi = 0.1$ (left) and $\xi = 1$ (right), where $\xi = y/\sqrt{R}$, compared to the exact solutions $Y_n(y)$ of the discrete recurrence relation (2) calculated for the same quotient $\xi = y/\sqrt{R}$ but for different values of R (and, therefore, different values of y).

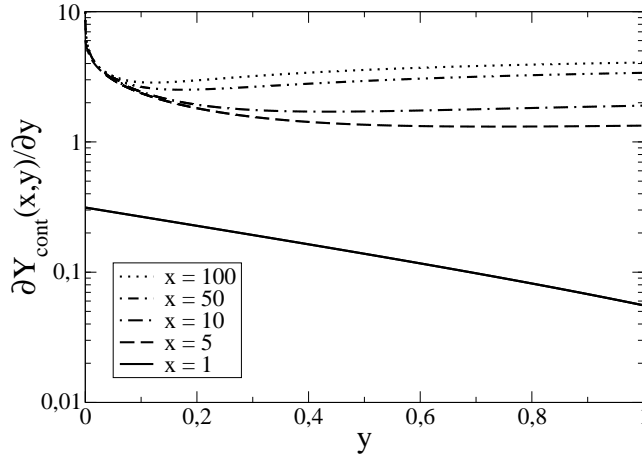


FIG. 2: Plots of $\partial Y_{cont}(x, y)/\partial y$ for (from lower to higher) $x = 1$, $x = 5$, $x = 10$, $x = 50$ and $x = 100$. All of them are positive for any $y > 0$, so all solutions of the form (9) are stable for any $y > 0$.

cumbersome, we prefer to show plots of the result for different values of x , which we collect in Fig. 2. It can be shown in general that $\partial Y_{cont}(x, y)/\partial y > 0$ for all $x > 0$, and therefore Eq. (9) is a stable solution of (2).

In order to check these results, we used the equations of motion of the model (1) in order

to simulate the dynamics of initial data given by (9) with small perturbations, and then monitored the evolution of this curves in time. Fixed boundary conditions at both ends of the simulated interval were used, in order to prevent the chain from spontaneously closing: We note that the global minimum of the hamiltonian (1) is the null solution. Therefore, in order to verify our results we had to restrict the simulations to the sector of open-chain solutions by choosing those boundary conditions. With that caveat, our simulations fully confirm the predicted stability of solutions. We stress that such solutions are the ones that are relevant to the mechanical denaturation problem, where the spontaneous closing of the chain is prevented by the force exerted on the open end.

IV. DISCRETE LIMIT OF THE PEYRARD-BISHOP MODEL

A. Solutions

The discrete limit of the PB model corresponds to letting $R \gg 1$, and can be obtained following a few steps. Using a telescopic summation of $Y_{n+1} - Y_n$, and noting the initial conditions $Y_0 = 0$ and $Y_1 = y$, Eq. (2) can be rewritten as

$$Y_{n+1}(y) = (n+1)y + R \sum_{k=1}^n (n+1-k) V'(Y_k(y)). \quad (11)$$

We now define

$$f_k(y) \equiv V'(Y_k(y)) = 2e^{-Y_k(y)} (1 - e^{-Y_k(y)}) = f_1(Y_k(y)). \quad (12)$$

These functions are plotted for different values of R in the discrete limit in Fig. 3. As can be seen, these f_k are very localized, their overlapping depending on R . In fact, in the discrete limit we are working on, which implies low overlapping of the curves, we can calculate the position of the maxima of each $f_k(y)$, and subsequently approximate $f_k(y)$ by the first function, $f_1(y)$, by writing

$$f_k(y) \simeq f_k^{(1)}(y) \equiv f_1(b_k y), \quad (13)$$

with

$$b_n = \frac{1}{2\sqrt{R(R+2)}} \left[\left(R+1 + \sqrt{R(R+2)} \right)^n - \left(R+1 - \sqrt{R(R+2)} \right)^n \right]. \quad (14)$$

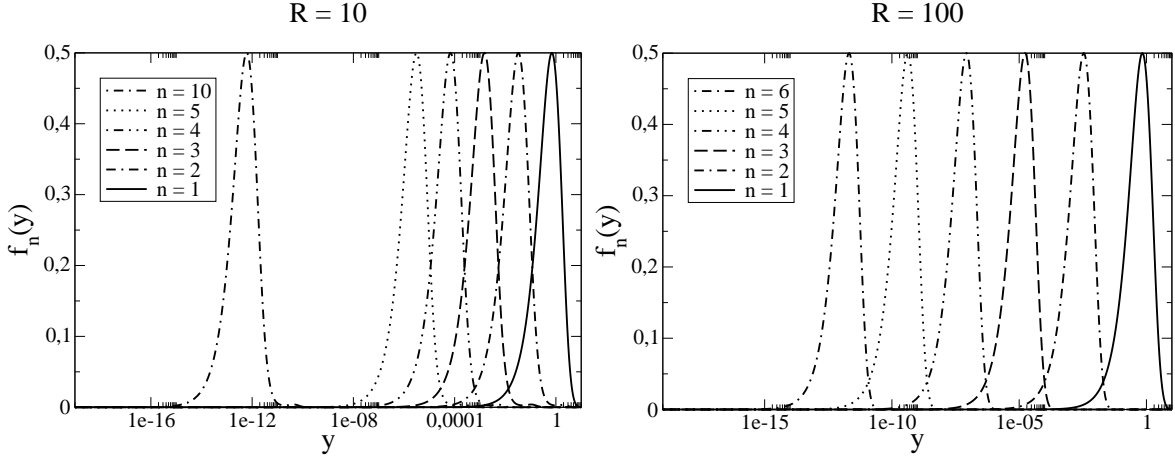


FIG. 3: Functions $f_n(y)$ for $R = 10$ (left) and $R = 100$ (right), for different values of n .

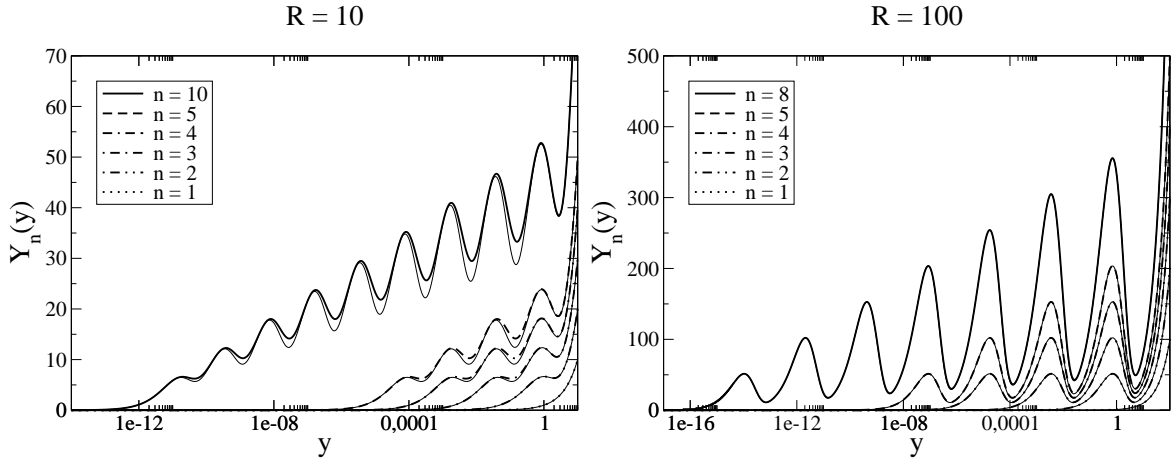


FIG. 4: Approximation $Y_n^{(1)}(y)$ (see Eq. (15)) vs. exact $Y_n(y)$, for $R = 10$ (left) and $R = 100$ (right), for different values of n . Exact solutions are drawn with thick lines, whereas the corresponding approximations are drawn in thin, solid lines.

This result allows us to obtain an analytic, approximate expression of the solutions for different y in the discrete limit. Substituting it in Eq. (11), we find that

$$Y_{n+1}^{(1)}(y) = (n+1)y + R \sum_{k=1}^n (n+1-k) f_k^{(1)}(y). \quad (15)$$

is a good approximation of the exact solution $Y_n(y)$ for large values of R . Figure 4 confirms the accuracy of this approximation: for $R \gtrsim 100$, the approximation is very accurate, whereas the smaller R the worse the approximation. For smaller values of R , the approxima-

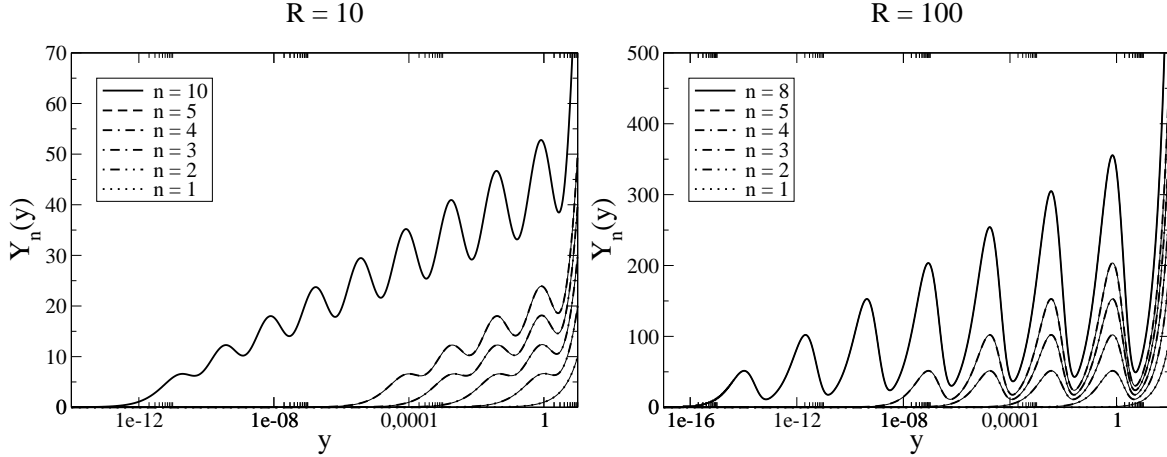


FIG. 5: Approximation $Y_n^{(2)}(y)$ (see Eq. (17)) vs. exact $Y_n(y)$, for $R = 10$ (left) and $R = 100$ (right), for different values of n . Exact solutions are drawn with thick lines, whereas the corresponding approximations are drawn in thin, solid lines.

tion can be improved by resorting to the next function, $f_2(y)$ instead of $f_1(y)$, as a substitute for the rest of the $f_k(y)$, by defining

$$f_k(y) \simeq f_k^{(2)}(y) \equiv f_2(y) \frac{b_k}{b_2} \quad (16)$$

for $k = 3, 4 \dots$, and approximating $Y_n(y)$ by

$$Y_{n+1}^{(2)}(y) = (n+1)y + nRf_1(y) + R \sum_{k=2}^n (n+1-k) f_k^{(2)}(y). \quad (17)$$

In this case, the approximation is even better than for $Y_n^{(1)}(y)$, and even for $R = 10$ the results are very close to the exact ones (see Fig. 5 for details).

The errors of these approximations depend on the value of R and n . For instance, $Y_n^{(1)}(y)$ is exact for $n = 1$ and $n = 2$, for any value of R , whereas $Y_n^{(2)}(y)$ is exact up to $n = 3$ for any R . For low values of n , the main difference between the exact $f_n(y)$ (which can be easily obtained numerically) and $f_n^{(1)}$ is located around the maxima of $f_n(y)$, with a maximum error $E_{max}^{(1)} \simeq 0.06$ for $R = 10$ and $E_{max}^{(1)} \simeq 0.006$ for $R = 100$. For the second order approximation based on $f_n^{(2)}$, the maximum error is $E_{max}^{(2)} \simeq 2.7 \cdot 10^{-3}$ for $R = 10$ and $E_{max}^{(2)} \simeq 3.2 \cdot 10^{-5}$ for $R = 100$; at the same time, another discrepant region, much less so than the main one, appears around the position of the maxima of $f_{n-1}(y)$. The same calculation can be done for higher orders of the approximating function, $f_n^{(k)}(y)$, and it can be seen that the

reduction of the error using $k + 1$ instead of k is at least of one order of magnitude. There is a computational limit near the precision of the machine, which does not allow us to check the validity of this assumption further than a certain k and n , depending of the value of R , but, as far as we know, it is reasonable to expect that the same behavior will take place for higher values of k and n . Therefore, we conjecture that higher orders of functions $f_k(y)$ can be used as approximations of $f_n(y)$, as $f_n(y) \simeq f_n^{(k)}(y)$, with

$$f_n^{(k)}(y) = f_k \left(y \frac{b(k')}{b(k)} \right) \quad (18)$$

for $n > k$, in order to obtain better approximations $Y_n^{(k)}(y)$ of the exact solution $Y_n(y)$, and that the error of an approximation of order k , $E_n^{(k)}(y) = Y_n(y) - Y_n^{(k)}(y)$, can be estimated as the difference

$$E_n^{(k)}(y) \simeq Y_n^{(k+1)}(y) - Y_n^{(k)}(y) + \mathcal{O}(E_n^{(k+1)}(y)), \quad (19)$$

with $E_n^{(k+1)}(y) \ll E_n^{(k)}(y)$.

B. Stability

The approximations defined in (15) and (17), as well as the ones mentioned in the above section allow us to calculate very accurately the solution $Y_n(y)$ for any value of n and y . This is important because in the exact, numerical calculation of Eqs. (2) and (11) there are problems for values of y close to zero, due to the numerical precision of the computer (see also the discussion below). Therefore, for analyzing the stability in the discrete limit, we proceed to use the approximations $Y_n^{(k)}(y)$ previously discussed. By this means, we can work with systems of much larger size than the ones that could be studied solving numerically the original recurrence relations. For comparison, in the study of stability we will show results for systems of small size, where the derivative $Y_n'(y)$ can be calculated without approximations for each n without high errors of the precision of the computer. In Fig. 6 we show the dependence of $\partial Y_n(y)/\partial \log_{10}(y)$ on function of the initial condition y , in logarithmic scale, for different values of the size of the system, N . We chose $\partial Y_n(y)/\partial \log_{10}(y)$ instead of $Y_n'(y)$ in order to obtain a smooth curve: The direct plot of $Y_n'(y)$ would make very difficult to observe the intervals with $Y_n'(y) > 0$. As the sign of both derivatives is the same for all $y > 0$, we have resorted the logarithmic one. With this change, a modulated "sinusoidal" structure reveals itself in Fig. 6 for each n , with $n - 1$ maxima and minima around $Y_n'(y) = 0$. From

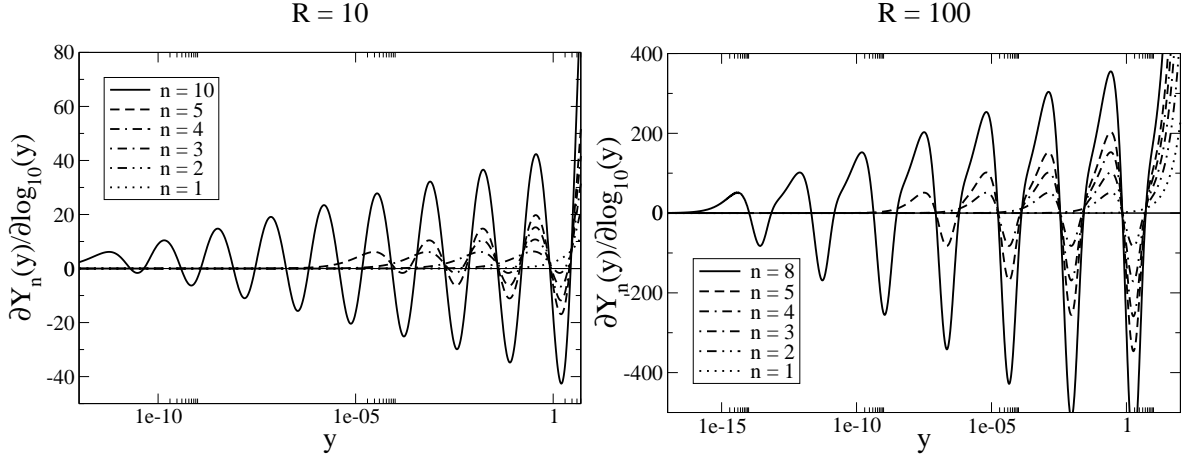


FIG. 6: Derivative of $Y_n(y)$ with respect to $\log_{10}(y)$ for different values of n and for $R = 10$ (left) and $R = 100$ (right), with logarithmic x axis. The stability region of a system of size N is the intersection of all the points that satisfy $\partial Y/\partial y > 0$ for $n = 1, 2, \dots, N + 1$. From the figures, we find that the stability region corresponds to the points that satisfy the condition for $n = N + 1$, as the stability region of a system of size N seems to be embedded in the stability region of a system of size $N - 1$ (see text for an explanation).

that figure, it is apparent that a new interval of instability for lower values of y appears in systems of size n as compared to systems of size $n - 1$. In addition to this, Fig. 6 also suggests that the set of unstable points of a system of size n contains the set of unstable points of a system of size $n - 1$. A plausibility argument for this statement goes as follows: Let us look at points that satisfy $Y'_n(y_0) = 0$, in the extremes of an interval of unstable points. Then, if $Y'_{n-1}(y_0) > 0$, it must be $Y'_{n+1}(y_0) < 0$ (see Eq. (6)), and therefore the interval of unstable points for a system of size n will be larger than for a system of size $n - 1$. This condition is satisfied by all the new unstable intervals that appear for each $Y_n(y)$, starting on $Y_2(y)$, and therefore, by induction, it can be applied to all systems. Therefore, all stable points of a system of size n are those who satisfy $Y'_{n+1}(y) > 0$.

As an independent check of the validity of the results shown in this section, we compared our results with the ones recently reported in [17]. By studying the discrete, stationary problem with fixed boundary conditions, they found eight stable and seven unstable solutions of a system of size $N = 28$. The specific boundary conditions they used were $Y_0 = 0$ and $Y_N = 80$ for $R = 10.1$. The exact $Y_n(y)$ and the approximate solution $Y_n^{(2)}(y)$ of that

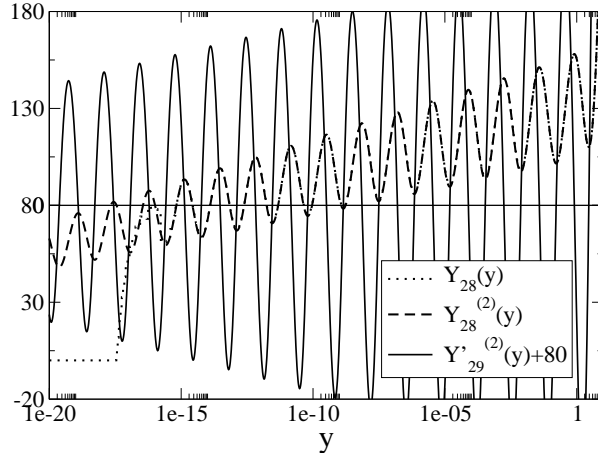


FIG. 7: Stable and unstable solutions given by approximation $Y_N^{(2)}$ for a system with $N = 28$ sites, $Y_0 = 0$ and $Y_N = 80$. The solutions are the intersections of the curves with the line $Y_{28} = 80$. It is necessary to study the sign of Y_{29}' on each solution in order to establish the stability of the solutions. Once again, $\partial Y_{29}(y)/\partial \log_{10}(y)$ is plotted for clarity. Our approximation gives eight stable and seven unstable solutions, exactly as in [17].

system are in Fig. 7. The plot now makes clear the precision problem we mentioned above, namely when we tried to calculate the exact, numerical solution for low values of y . On the other hand, the approximate solution $Y_n^{(2)}(y)$ was calculated without any problem in a wide range of y . It is also shown that $Y_n^{(2)}(y)$ gives the same number of both stable and unstable solutions as in [17] (see explanation in caption), which implies that the structure of peaks of $Y_n(y)$ gives a good explanation of the number and structure of solutions. We think that this method can be applied for larger systems with the way to estimate errors that we explained in this section.

V. CONCLUSIONS

In this paper, we have reported a study of the stationary solutions of the PB model, obtaining exact and analytical approximations of the continuum and the discrete limit. We have been able to obtain all the stationary solutions and to classify them according to their stability by considering the stationary equation as an initial value problem. We have also found that, in the discrete limit, the exact solutions can be approximated to the desired

degree of accuracy by using the functions $f_k(y)$ as explained above. We have compared our results obtained in the discrete limit with [17] finding a very good agreement with the number of stable and unstable solutions of a PB system with fixed boundary conditions, thus giving an explanation of the multiple solutions of the problem and the stability. In fact, our results show that every solution of the initial value problem, which is unique for every choice of y , corresponds to exactly one of the problem with fixed boundary conditions [17], which does not have a unique solution. This is the reason why the picture we are providing here is much more comprehensive and allows to understand fully the space of solutions of the problem. On the other hand, the method explained in this paper to obtain stable solutions of a system of size N and opening L allows to work with larger systems, as solutions and their stability are calculated by evaluating a function, instead of numerically (as in [17], with $N = 28$). We also believe that this study may be extended to the more accurate description of DNA given by the Peyrard-Bishop-Dauxois model [6], where the coupling between two consecutive bases of the DNA molecule has an anharmonic term that affects the general behavior of the openings [8, 18].

As stated in the introduction, this stems from previous studies in the sine-Gordon (Englander) model of DNA [11, 12], where the relation between the dynamics of soliton-like excitations and the inhomogeneity of the DNA sequence was studied. In fact, what we are reporting here is only the first step towards the study of an effective potential that may explain the dynamics of these stationary, stable solutions in presence of heterogeneities in the sequence and an external force. Once an analytical expression of the stationary solutions of the model is found, as we have just done, we will resort to a collective coordinate technique to find an *effective potential* description of the dynamics. The final aim of such a program is to find out whether this approach allows to identify important sites from the genomic viewpoint along any given sequence. While work along these lines is in progress, we believe that the richness of the structure of the stationary solutions we have found and their stability is of interest in itself and can motivate further research in these and related models. Finally, we believe our solutions can be exploited to analyze the statistical mechanics of the PB model along the lines of [17, 19], in particular because of the advantage of having an approximate, analytical expression.

Acknowledgments

We thank Michel Peyrard and Fernando Falo for many discussions about DNA and domain walls. This work has been supported by the Ministerio de Educación y Ciencia of Spain through grants BFM2003-07749-C05-01, FIS2004-01001 and NAN2004-09087-C03-03. S.C. is supported by a fellowship from the Consejería de Educación de la Comunidad Autónoma de Madrid and the Fondo Social Europeo.

-
- [1] E. Fermi, J. R. Pasta and S. Ulam, Los Alamos Report LA-UR-1940 (1955); reprinted in *Collected Papers of Enrico Fermi*, edited by E. Segré (University of Chicago, Chicago, 1965).
 - [2] A. C. Scott, *Nonlinear Science* (Oxford University, Oxford, 1999).
 - [3] S. W. Englander, N. R. Kallenbach, A. J. Heeger, J. A. Krumhansl, and A. Litwin, Proc. Natl. Acad. Sci. USA **77**, 7222 (1980).
 - [4] L. V. Yakushevich, *Nonlinear Physics of DNA*, 2nd edition (Wiley-VCH, Weinheim, 2004).
 - [5] M. Peyrard and A. R. Bishop, Phys. Rev. Lett. **62**, 2755 (1989).
 - [6] T. Dauxois, M. Peyrard, and A. R. Bishop, Phys. Rev. E **47**, R44 (1993); T. Dauxois and M. Peyrard, Phys. Rev. E **51**, 4027 (1995).
 - [7] A good summary of the experimental advances can be found in the collection of articles *The Double Helix — 50 Years*, Nature **421**, 396 (2003).
 - [8] G. Kalosakas, K. Ø. Rasmussen, A. R. Bishop, C. H. Choi, and A. Usheva, Europhys. Lett. **68**, 127 (2004); C. H. Choi, G. Kalosakas, K. Ø. Rasmussen, M. Hiromura, A. R. Bishop, and A. Usheva, Nuc. Acids Res. **32**, 1584–1590 (2004).
 - [9] T. S. van Erp, S. Cuesta-López, J.-G. Hagmann, and M. Peyrard, Phys. Rev. Lett. **95**, 218104 (2005).
 - [10] S. Ares, N. K. Voulgarakis, K. . Rasmussen, and A. R. Bishop Phys. Rev. Lett. **94**, 035504 (2005).
 - [11] S. Cuenda and A. Sánchez, Fluct. Noise Lett. **4**, L491 (2004).
 - [12] S. Cuenda and A. Sánchez, Phys. Rev. E **70**, 51903 (2004).
 - [13] M. Peyrard, Nonlinearity **17**, R1 (2004).
 - [14] M. Salerno, Phys. Rev. A **44**, 5292 (1991).

- [15] M. Salerno, Phys. Lett. A **167**, 49 (1992).
- [16] M. Salerno and Yu. S. Kivshar, Phys. Lett. A **193**, 263 (1994).
- [17] N. Theodorakopoulos, M. Peyrard, and R. S. MacKay, Phys. Rev. Lett. **93**, 258101 (2004).
- [18] A. Campa and A. Giansanti, Phys. Rev. E **58**, 3585 (1998).
- [19] H. Qasmi, J. Barr and T. Dauxois, preprint [arXiv:cond-mat/0407662](https://arxiv.org/abs/cond-mat/0407662) (2004).